

University of Texas Rio Grande Valley

ScholarWorks @ UTRGV

Physics and Astronomy Faculty Publications
and Presentations

College of Sciences

2005

Electric-field generated by the combustion of titanium in nitrogen

Karen S. Martirosyan

The University of Texas Rio Grande Valley

Mona Setoodeh

Dan Luss

Follow this and additional works at: https://scholarworks.utrgv.edu/pa_fac

 Part of the [Astrophysics and Astronomy Commons](#), and the [Physics Commons](#)

Recommended Citation

Martirosyan, Karen S.; Setoodeh, Mona; and Luss, Dan, "Electric-field generated by the combustion of titanium in nitrogen" (2005). *Physics and Astronomy Faculty Publications and Presentations*. 355.
https://scholarworks.utrgv.edu/pa_fac/355

This Article is brought to you for free and open access by the College of Sciences at ScholarWorks @ UTRGV. It has been accepted for inclusion in Physics and Astronomy Faculty Publications and Presentations by an authorized administrator of ScholarWorks @ UTRGV. For more information, please contact justin.white@utrgv.edu, william.flores01@utrgv.edu.

Electric-field generated by the combustion of titanium in nitrogen

K. S. Martirosyan,^{a)} Mona Setoodeh, and Dan Luss^{b)}

Department of Chemical Engineering, University of Houston, Houston, Texas 77204

(Received 24 March 2005; accepted 30 June 2005; published online 6 September 2005)

A short temporal electrical impulse (duration of 30–150 ms) was generated during the nitridation of mixtures of titanium and titanium nitride by a high temperature moving reaction front. The maximum voltage and current were generated in the combustion front region, in which the conversion of Ti to TiN was incomplete. The electric field (voltage up to 2 V and current up to 60 mA) decayed and vanished before the maximum combustion temperature was attained. The generation of an electric field during a rapid high-temperature nitridation is most probably due to the different diffusion velocities of charge carriers through the growing titanium nitride shell during the initial stage of the reaction. When the reactant mixture contained a high percentage of pure titanium (larger than 60 wt %), partial melting led to irreproducibility in the amplitude and duration of the electrical signal. © 2005 American Institute of Physics. [DOI: 10.1063/1.2007847]

INTRODUCTION

Many experimental and theoretical investigations have significantly enhanced our understanding of the kinetics and mechanisms of metal combustion in different gas environments (O₂, N₂, H₂, or their mixture). The combustion of metal particles in oxygen may generate an electromagnetic field in and around the sample.^{1–5} For example, electrical voltage and current of about 2 V and 100 mA were measured during the initial stage of combustion in oxygen of large ($\varnothing \sim 0.8$ mm) single metal particles of Zr, Ti, Fe, and Ni.⁶ The different diffusion fluxes of positive and negative charge carriers through a mixed ionic-electronic conducting oxide shell was the main cause for the generation of this temporal electrical field.^{6,7}

Almost all previous studies of electrical-field formation during high-temperature gas-solid combustion involved oxidation reactions. Only two studies were concerned with electric-field formation during nitridation.^{8,9} A bipolar electrical signal with maximum amplitude of about 80 mV was generated during the nitridation of titanium between two electrodes located 50 mm apart in the direction of the propagating temperature front.⁸ The two electrodes were exposed to different temperatures, nitrogen pressures, nitridation degrees, and electric resistances when the signal was measured. These studies did not determine the relations between the formation of the local electrical potential, local combustion temperature, and product conversion. The mechanism of the electrical-field formation during metal nitridation by combustion synthesis is not established at present, nor is it possible to predict its magnitude, impact, and potential applications.

The combustion synthesis of titanium nitride has been studied extensively^{10–14} owing to its desirable properties, such as thermal stability, high hardness, and relatively high electrical conductivity. Time-resolved x-ray diffraction (TRXD) showed that the first step in this nitridation was an

$\alpha \rightarrow \beta$ transition of the Ti, followed by formation of TiN.¹⁰ A solid solution of nitrogen in titanium formed during the first 2 s of interaction. The nitridation of the titanium was completed in about 6 s after the propagation of the combustion front. Quenching the combustion front over a wide range of nitrogen pressures (0.1–20 MPa),^{11,12} showed that the titanium nitridation was incomplete in the combustion front. Several complex phase transitions, which depended strongly on the gas pressure, occurred during the nitridation. It was suggested that a thin surface layer of TiN and an unsaturated solid solution form in the propagating high-temperature front. This nitride surface layer is formed and dissolved as the solution becomes saturated.¹⁵ The growth rate of TiN formed in high-temperature nitridation is controlled by nitrogen diffusion.^{11,12} Prediction of the characteristics of the electric field evolved during the nitridation requires knowledge of the mechanism by which nitrogen diffuses through titanium or TiN, as this determines if and which charge carriers form during that transport. However, there exists no established mechanism of nitrogen diffusion during the nitridation.

We studied the temporal evolution of electrical field and temperature rise during the nitridation of Ti in order to enhance our knowledge and understanding of this phenomenon and to enable the development of models predicting its characteristics. Since the combustion temperature of pure Ti powder in nitrogen is much higher than the melting temperatures of the electrodes and thermocouple, we used mixtures of Ti and TiN as the reactants. The experimental technique described in Ref. 16 was used to measure simultaneously the local electrical potential and temperature.

EXPERIMENTAL SYSTEM AND PROCEDURE

Figure 1 is a schematic of the top view of the experimental system; (A-A) the cross section of the ceramic boat is shown on the side. The temperature and electrical voltage/current signals were measured by a multichannel data-acquisition board (Omega, Inc.) and recorded on a personal computer (PC). The electric voltage/current were measured

^{a)}Electronic mail: kmartirossian@uh.edu

^{b)}Electronic mail: dluss@uh.edu

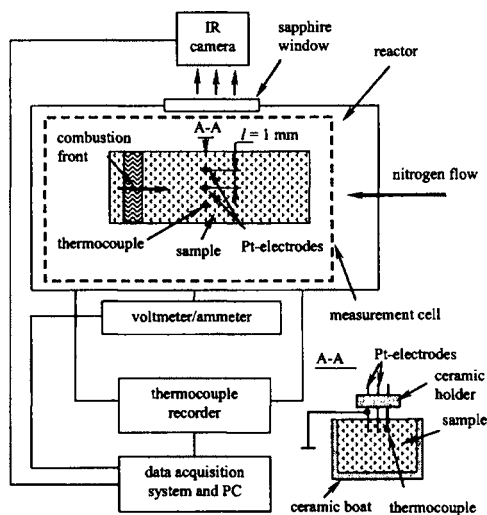
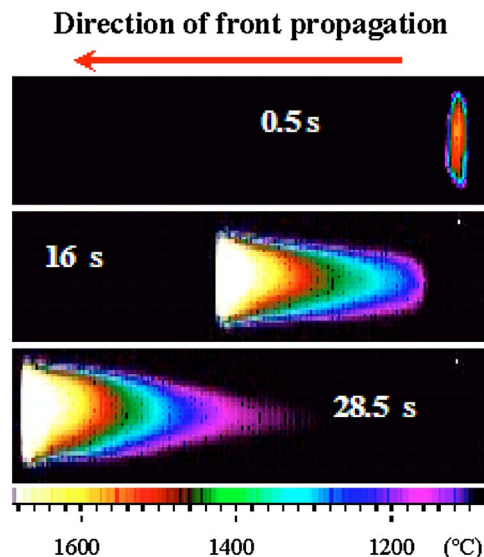


FIG. 1. Schematic of the experimental system.

by two Pt electrodes ($\varnothing \sim 0.1 \text{ mm}$) that were inserted at a depth of $\sim 1\text{--}2 \text{ mm}$ from the sample surface and located at a distance of 1 mm from each other in a plane perpendicular to the direction of the moving planar combustion front. Thus, for the two electrodes the combustion front was planar, even when the front was somewhat distorted below the surface and around the ends of sample. The distance between the two electrodes l was ten times smaller than their distance from the boat wall in order to prevent distortion of the front by the reactor wall.

The electrodes were directly connected to the input of a voltmeter/ammeter. The impedance during the voltage and current measurements were $0.25 \text{ M}\Omega$ and 0.1Ω , respectively. The electric potential along the planar combustion front is uniform. Therefore, in order to measure the electric potential of the combustion front with reference to the ground one electrode was set as the earth. The temperature was measured by a *S*-type (Pt–Rh) or *C*-type (W/Rh) thermocouple of about 0.1-mm diameter. The enthalpy of the reaction $\text{Ti} + 1/2\text{N}_2 \rightarrow \text{TiN}$ is about $\Delta H_{298}^0 = -334.4 \text{ kJ/mol}$ and the adiabatic combustion temperature is about 4602 K .¹⁷ It was essential to decrease the reaction temperature to protect the Pt electrodes and thermocouple from melting. This was accomplished by mixing titanium and TiN powders (99.5% pure, Alfa Aesar Company). The average particle sizes of the Ti and TiN were ~ 12 and $3 \mu\text{m}$, respectively. The reactant powders with different ratios of Ti/TiN were mixed for 30 min in a ball mill machine (CertiPrep, Inc). About 10 g of the loose reactant mixture (relative density $\cong 0.35$) was placed into a 8-cm -long ceramic boat in quartz reactor fed by nitrogen (99.99%) at a flow rate of up to 10 l/min (measured under atmospheric pressure and room temperature). The reactant's mixture was ignited by an electrically heated coil, the width of which ($\sim 12 \text{ mm}$) was almost equal to that of the boat to ensure formation of a planar front. The current to the heating coil was terminated immediately after ignition to avoid electrical disturbance during the measurements.

An IR digital video camera (60 frame/s, Indigo Systems) with high-temperature germanium filter was used to

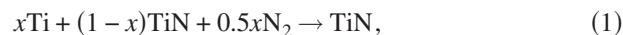
FIG. 2. (Color online) Temporal IR thermal images of the sample surface during the combustion synthesis of titanium nitride ($x=0.5$).

follow the shape, temperature, and the velocity of the combustion front. The IR camera was calibrated to measure temperatures up to $2000 \text{ }^\circ\text{C}$ using an electrically heated wolfram coil and a W/Rh thermocouple.

The product composition and microstructure were analyzed by x-ray diffraction (XRD) (Siemens D5000; Cu $K\alpha$ radiation source) and scanning electron microscopy (SEM) (JEOL JAX8600, Japan). The mass fraction of each phase in the combustion product was determined by the reference intensity ratio (RIR) method. Crystal cell parameters were calculated and refined applying linear regression procedures (Philips APD1700 software) to the measured peak positions of all the major reflections.

EXPERIMENTAL RESULTS

We measured the temporal electric signal generated during the nitridation of mixtures of titanium and titanium nitride powder by the reaction:



where x is dilution coefficient with $0.5 \leq x \leq 0.8$. At a dilution of $50 \text{ wt } \%$, neither Ti nor its products melted during the gas-solid nitridation reaction. The reaction temperature of mixtures with $x > 0.6$ exceeded $1900 \text{ }^\circ\text{C}$, causing melting of the titanium particles.

Figure 2 shows typical infrared (IR) images during the synthesis at $x=0.5$. IR thermal images of the sample surface showed that the combustion front was planar at the center of the sample, where the electrodes and thermocouple were located. It propagated with a constant velocity of about 2.8 mm/s and its maximum temperature was about $1700 \text{ }^\circ\text{C}$. The temporal electric voltage and temperature generated during the combustion synthesis of TiN are shown in Fig. 3. An electrical voltage formed when the moving front temperature was about $1300 \text{ }^\circ\text{C}$. The voltage and current attained their maximum values ($\sim 0.85 \text{ V}$ and $\sim 20 \text{ mA}$) at a temperature of $\sim 1400 \text{ }^\circ\text{C}$. The voltage was annihilated at about

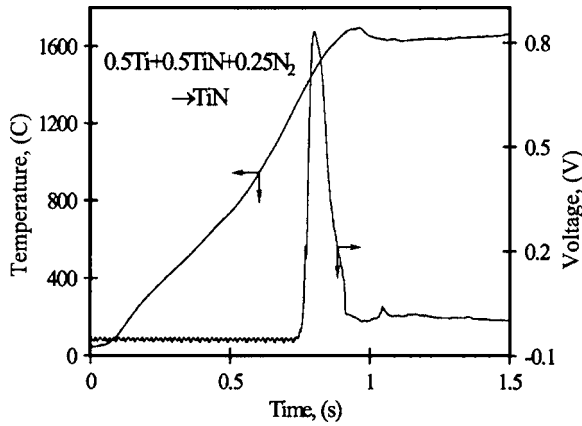


FIG. 3. Temporal temperature and electric voltage generated by a planar combustion front. The distance between two Pt electrodes ~ 1 mm ($x=0.5$).

1600 °C, i.e., before the maximum combustion temperature of 1700 °C was attained. The duration of the electric field of 150 ms was much shorter than that of the temperature rise (~ 1 s). Each experiment was repeated five times and the electrical voltage and current signals were reproducible within $\pm 10\%$ during the combustion synthesis of TiN at $x=0.5$.

An increase in the content of Ti in the mixture increased the combustion temperature and the maximum voltage/current amplitude. However, the high reaction temperature in mixtures containing more than 60-wt % Ti, caused a large irreproducibility in the amplitude and duration of the electrical signals. Figure 4(a) shows the two electric signals ob-

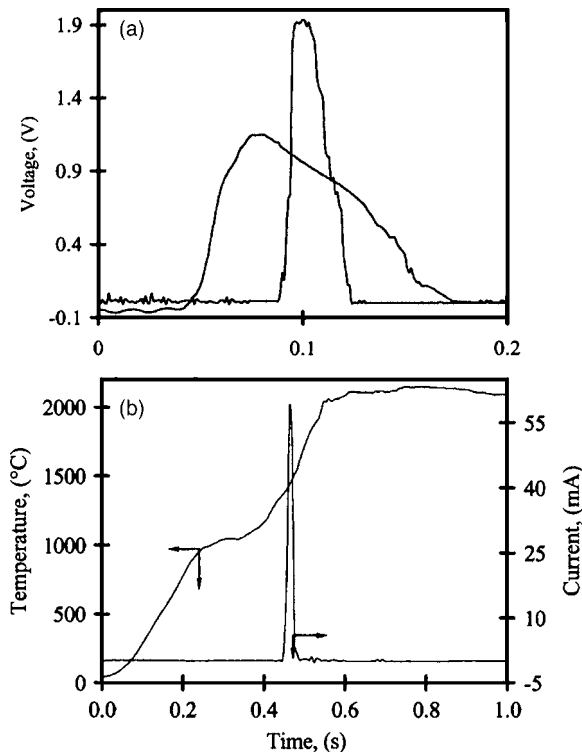


FIG. 4. (a) Temporal electric voltage generated by two experiments conducted under the same experimental conditions for $x=0.8$; and (b) Evolution of temporal electrical current and temperature for $x=0.8$. The distance between the two Pt electrodes ~ 1 mm.

TABLE I. The thermal wave characteristics and electric voltage and current generated during combustion synthesis of TiN for various compositions.

Dilution coefficient x	Combustion velocity (mm/s)	Maximum combustion temperature (°C)	Maximum voltage (V)	Maximum current (mA)
0.5	2.8	1700	0.85	20
0.6	3.4	1890	0.9–1.5	20–36
0.7	3.9	2020	1–1.8	24–40
0.8	4.2	2150	1.1–2.0	30–60

tained for two repeated experiments carried out under identical conditions for a mixture with $x=0.8$. The maximum electrical voltage and current in these two experiments changed from 1.1 to 2.0 V and 30 to 60 mA, respectively. Moreover, the signal duration was 30 ms in one experiment and 100 ms in the second. The electrical signals were generated and annihilated well before the combustion temperature attained its maximum [Fig. 4(b)]. The thermal wave characteristics and electric signal measurements during combustion synthesis of TiN for various compositions are summarized in Table I. The large irreproducibility between repeated experiments at $x \geq 0.6$ is probably caused by the molten Ti in the back of the moving combustion front. It causes movement of the particles located between the two electrodes and affects the electrical signal reproducibility.

An electrode and a thermocouple were placed at about 1 mm above the sample's surface (the ground electrode was still inside the sample) to measure the electrical gradient in the gas phase around the high-temperature combustion front. Figure 5 shows that the electrical signal in the gas phase exhibited a very weak smooth signal with a maximum amplitude of about 3 mV. The amplitudes of the voltage in the gas phase during the synthesis of TiN at $x=0.5$ and 0.6 were about 1.5 and 2.8 mV, respectively. The behavior of these signals was similar to that obtained for $x=0.8$. The voltage increased monotonically with the temperature. The electrical signal in the gas phase around the combustion front was negligible compared with the generated electrical signal on the surface of particles.

A scanning electron micrograph [Fig. 6(a)] of the grain

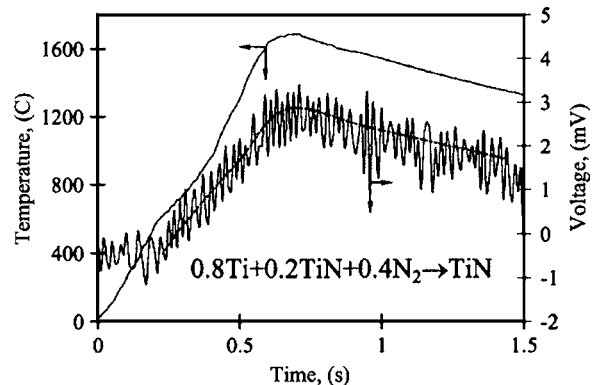


FIG. 5. Temporal electric voltage and temperature generated in the gas phase around the sample for $x=0.8$. Ground electrode was inside the sample. The second electrode and thermocouple were located 1 mm above the sample.

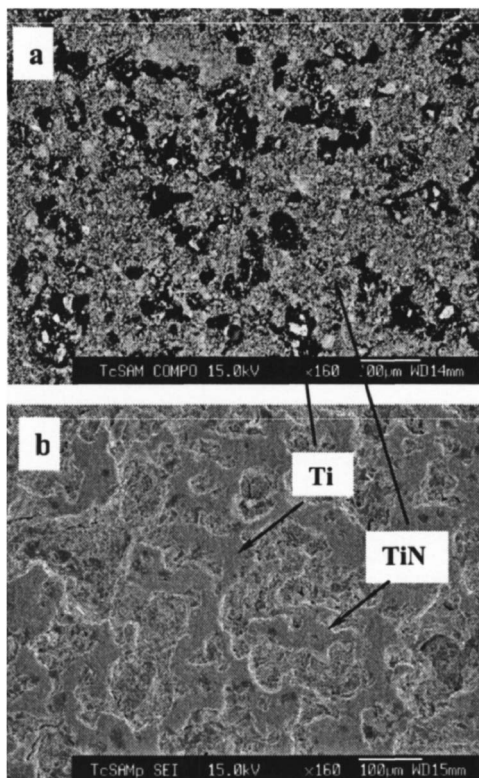


FIG. 6. The microstructure of combustion product produced from a mixture with (a) $x=0.5$, and (b) $x=0.8$.

structure and the agglomeration of titanium nitride particles (smaller than $1-2 \mu\text{m}$) indicated that no melting occurred during the nitridation when $x=0.5$. Image processing of the micrograph (OPTIMAS 6.0 software) revealed the presence of 3% unreacted Ti particles (white spots in Fig. 6(a) micrograph) with a size of about $10 \mu\text{m}$ around the center of the sample. Nitridation of mixtures containing more than 60-wt% Ti caused partial melting of the Ti, which, in turn, decreased the conversion. A micrograph of a sample containing 80-wt% Ti [Fig. 6(b)] revealed a continuous liquid Ti matrix, surrounded by TiN layers at the edge of the pores.

XRD analysis of the combustion products at $x=0.5$ (Fig. 7) showed that the conversion of titanium to titanium nitride was complete near the surface, but only 97% at the center of the product. The synthesized titanium nitride has a NaCl-type cubic crystal ($Fm3m$) structure. Its lattice parameter, calculated from the patterns of the strongest peaks [200], [111], and [220] of 4.239 \AA , closely agreed with the reported values.¹⁸

DISCUSSION

Previous studies indicated that the nitridation of Ti was not completed in the combustion zone, i.e., before the maximum temperature was reached, and that it was completed in the post combustion region.¹⁰⁻¹² In all our experiments the maximum voltage (measured by electrodes inside the sample) was obtained before the maximum temperature was achieved [Figs. 3 and 4(b)]. Thus, the electrical signal was

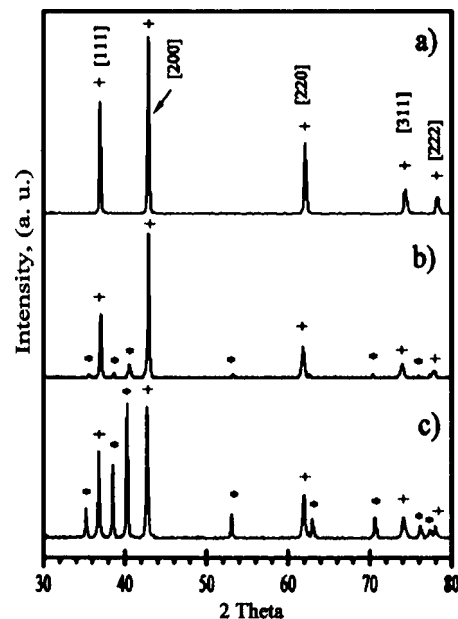


FIG. 7. Powder x-ray diffraction of (a) sample surface, (b) center of sample, and (c) initial mixture, $x=0.5$. Key: (*) Ti, and (+) TiN.

generated when the titanium was only partially converted to TiN and the particles consisted of a Ti core surrounded by a shell of TiN.

The experiments indicate that if the maximum combustion temperature exceeds $\sim 1700 \text{ }^\circ\text{C}$ a large irreproducibility of the electrical signal between repeated experiments occurs. This is due to the short distance between the region in which melting occurs and that at which the electrical current decays. When the temperature at the reaction zone considerably exceeds the titanium melting temperature of $1660 \pm 10 \text{ }^\circ\text{C}$, the flow of titanium in the back of the moving front can cause movement of the particles located between the electrodes, leading to irreproducibility of the electrical signal. For example, at $x=0.8$ the combustion front moves at a velocity of about 4.2 mm/s . The time span between the generation and extinction of the signal, and achieving the maximum combustion temperature is about 0.2 s [Fig. 4(b)]. Therefore, the distance between particles located between the electrodes and those at the maximum combustion temperature of about $2150 \text{ }^\circ\text{C}$ is less than 1 mm ($4.2 \text{ mm/s} \times 0.2 \text{ s} = 0.84 \text{ mm}$).

Three established mechanisms may generate an electrical field during a high-temperature gas-metal reaction: thermoelectric phenomenon (TP) or Seebeck effect, high-temperature electron thermal emission (TE),¹⁹ and differential diffusion of charge carriers through a product layer.

A temperature difference at the junction of two dissimilar metals produces a thermoelectromotive force E , satisfying the relation

$$E = \tilde{k}(T_1 - T_2), \quad (2)$$

where T_1 and T_2 are the combustion and initial (room) temperatures, respectively; \tilde{k} is a coefficient that depends on the two metals. The voltage generated by TP between Ti, TiN, and Pt, present in our system, is estimated to be smaller than

20 mV at 1800 K (average temperature at which the electrical signals existed). The thermoelectric effect in either *S*- or *C*-type thermocouple generates an electric voltage of the order of 20–35 mV.²⁰ The measured electric voltage in our experiments was significantly higher in the range of 0.8–2 V (Figs. 3 and 4). Thus, thermoelectric phenomenon was not a dominant factor in the electric-field formation in our experiments.

The current density (J_e) generated by thermal emission from a homogeneous surface is predicted by the Richardson-Dushman relation to be¹⁹

$$J_e = (1 - \bar{k})A_0 T^2 \exp(-\phi/KT), \quad (3)$$

where \bar{k} is the electron reflection coefficient, $A_0 = 4\pi me^2/h^3 = 1.204 \times 10^6 \text{ A m}^{-2} \text{ K}^{-2}$, ϕ is the solid work function, e is the electron charge, m is the electron mass, k is Boltzman's constant, and h is Planck's constant. The work function for α Ti, β Ti, Pt, and TiN is 3.95, 3.65, 5.32, and 3.75 eV, respectively. At a temperature of 2000 K the maximum calculated thermal emission current density for $\bar{k}=0$ and $\phi=3.65$ eV is about 0.3 A/cm². The maximum measured current density between two electrodes with an area of $2 \times 10^{-3} \text{ cm}^2$ during our experiment was about 30 A/cm², exceeding by two orders of magnitude those predicted by Eq. (3). Moreover, for atmospheric gas surrounding the electron reflection coefficient \bar{k} exceeds zero, which further decreases the predicted value of TE current density.

Both the electric voltage generated by the thermoelectric phenomenon and the current produced by the thermal emission increased monotonically with temperature. The weak signals generated by the TE effects can be seen in Fig. 6. However, when the electrodes were located inside the samples (Figs. 3 and 4) the duration of the signals was much shorter than that of the temperature rise and their maximum values were obtained before the sample attained its maximum temperature. Thus, neither thermoelectric nor thermal emission phenomena were the main source of the electrical field formed in our experiments. Thus, we conjecture that the electrical field was generated mainly by the different rates of diffusion of charge carriers through the product layer.

The mechanism by which nitrogen diffuses through titanium or TiN during high-temperature titanium nitridation has not yet been established. This information is essential for determining if and which charge carriers form during this reaction. It was reported^{21,22} that nitrogen vacancies form in δ TiN when the nitrogen concentration is lower than the stoichiometric composition, while titanium vacancies form when the nitrogen concentration exceeds the stoichiometric composition. It was suggested that nitrogen vacancies are the principal defects in the nitride layer.²³ Trace experiments revealed that the δ -TiN layer grew by nitrogen atom diffusions. The formation of nitrogen vacancies in titanium nitrides is governed by the reaction



where N^x denotes a nitrogen atom and V^x a vacancy in the nitrogen site. The gaseous nitrogen is adsorbed as a very thin

layer on the titanium particle's surface via the reversible reaction



At the same time, electron-hole pairs are generated on the particle surface via thermal ionization $e^- + h^+ \leftrightarrow \text{nil}$. Accordingly, in the absence of interaction between defects, the concentration of charge carriers on the solid surface is determined by the reaction,



The low enthalpy ~ 0.213 eV (Ref. 24) of reaction (6) supports the conjecture that negative nitrogen ions (N^-) form on the surface of the titanium particles and diffuse through the growing shell of TiN. They rapidly react with titanium at the shrinking metal core. The nitrogen diffusion flux determines its rate of consumption at the shrinking metal core, and the growth rate of the exterior nitride shell. Thus, during the nitridation nitrogen ions, vacancies and electron-hole pair diffuse through the growing titanium nitride shell. A double charge layer is formed on the surface of individual particles due to the different diffusive velocities of the charge carriers across the growing product shell. The magnitude of the electrical signal depends on the ratio of the diffusion fluxes of the positive and negative charge carriers.

CONCLUSIONS

The experiments suggest that a temporal electric voltage and current form during the high-temperature titanium nitridation due to different diffusion velocities of charge carriers (negative nitrogen ions, positive nitrogen vacancies in TiN, and electron-hole pair) through a growing titanium nitride shell. The transient electrical signal formed during the initial stage of the combustion, before the maximum combustion temperature was attained and before the titanium nitridation was completed. Strictly "solid" nitridation experiments of mixtures containing Ti and 50-wt % TiN proceeded as gas-solid reactions and were reproducible. Partial melting occurred in mixtures containing more than 60 wt % of Ti due to higher combustion temperatures. This led to irreproducibility of the electrical measurements.

A reliable predictive model of the electrical-field formation during the nitridation of a powder requires knowledge and understanding of the nitridation mechanism of a single spherical pellet. This information about this complex process may be attained by conducting single pellet experiments. Understanding of this electrical-field evolution may be of importance also in other high-temperature processes encountered in combustion, rockets, and some explosives.

ACKNOWLEDGMENTS

We acknowledge the financial support of this research by the National Science Foundation, and the Materials Research Science and Engineering Center at the University of Houston.

¹A. G. Merzhanov, S. O. Mkrtychyan, M. D. Nersesyan, P. B. Avakyan, and

- ¹K. S. Martirosyan, Dokl. Akad. Nauk Republic of Romania **93**, 81 (1992).
- ²M. D. Nersesyan, J. R. Claycomb, Q. Ming, J. H. Miller, J. T. Richardson, and D. Luss, Appl. Phys. Lett. **75**, 1170 (1999).
- ³K. S. Martirosyan, J. R. Claycomb, G. Gogoshin, R. A. Yarbrough, J. H. Miller, Jr., and D. Luss, J. Appl. Phys. **93**, 9329 (2003).
- ⁴I. Filimonov and D. Luss, AIChE J. **50**, 2287 (2004).
- ⁵K. S. Martirosyan, J. R. Claycomb, J. H. Miller, Jr., and D. Luss, J. Appl. Phys. **96**, 4632 (2004).
- ⁶K. S. Martirosyan, I. A. Filimonov, M. D. Nersesyan, and D. Luss, J. Electrochem. Soc. **150**, J9 (2003).
- ⁷K. S. Martirosyan, I. A. Filimonov, and D. Luss, AIChE J. **50**, 241 (2004).
- ⁸Y. G. Morozov, M. V. Kuznetsov, M. D. Nersesyan, and A. G. Merzhanov, Dokl. Akad. Nauk **351**, 780 (1996).
- ⁹V. A. Kudryashov, A. S. Mukasyan, and I. A. Filimonov, J. Mater. Synth. Process. **4**, 353 (1996).
- ¹⁰I. O. Khomenko, A. S. Mukasyan, V. I. Ponomarev, I. P. Borovinskaya, and A. G. Merzhanov, Combust. Flame **92**, 201 (1993).
- ¹¹S. Deevi and Z. A. Munir, J. Mater. Res. **5**, 2177 (1990).
- ¹²M. Eslamloo-Grami and Z. A. Munir, J. Am. Ceram. Soc. **73**, 1235 (1990).
- ¹³A. E. Pelek, A. S. Mukasyan, and A. Varma, Ind. Eng. Chem. Res. **38**, 793 (1999).
- ¹⁴E. L. Dreizin, Prog. Energy Combust. Sci. **26**, 57 (2000).
- ¹⁵H. Rode and V. Hlavacek, Combust. Sci. Technol. **99**, 161 (1994).
- ¹⁶K. S. Martirosyan, I. A. Filimonov, and D. Luss, Int. J. Self-Propag. High-Temp. Synth. **11**, 325 (2002).
- ¹⁷J. A. Puszynski, in *Carbide, Nitride and Boride Materials Synthesis and Processing*, Thermochemistry and Kinetics, edited by A. W. Weimer (Chapman and Hall, London, 1997), p. 183.
- ¹⁸H. J. Goldschmidt, *Interstitial Alloys* (Butterworths, London, 1967), p. 296.
- ¹⁹I. S. Grigoriev and E. Z. Melikhov, *Handbook of Physical Quantities* (CRC, Boca Raton, FL, 1997), p. 1548.
- ²⁰G. W. Burns, M. G. Seroger, G. F. Strouse, M. C. Croarkin, and W. F. Guthrie, National Institute of Standards and Technology (U.S.) (1993), p. 175.
- ²¹L. Wei, C. Dosho, Y.-K. Cho, S. Tanigawa, and K. Hinode, Jpn. J. Appl. Phys., Part 2 **29**, L1500 (1990).
- ²²Y. Maruyama, J. Hojo, O. Iwamoto, and A. Kato, J. Less-Common Met. **53**, 265 (1977).
- ²³K. Shinozuka, M. Susa, T. Maruyama, and K. Nagata, Defect Diffus. Forum **143-147**, 1237 (1997).
- ²⁴H. Massey, *Negative Ions*, 3rd ed. (Cambridge University Press, UK, 1976), p. 741.